14th International Symposium on Turbulence and Shear Flow Phenomena (TSFP14)
Heidelberg, Germany, July 28–31, 2026

ANALYSIS OF THE FLOW OVER CHECKERBOARD HETEROGENOUS ROUGHNESS USING PARTICLE TRACKING VELOCIMETRY AND HOT WIRE ANEMOMETRY

Tomos Rich
Institute of Fluid Mechanics (ISTM)
Karlsruhe Institute of Technology
Kaiserstraße Karlsruhe 76131
tomos.rich@kit.edu

Patricia Sujar-Garrido
Department of Engineering Mechanics
KTH Royal Institute of Technology
Stockholm, Sweden
pasg@kth.se

Carola Schmidt, Jonathan Neuhauser, Jochen Kriegseis, Bettina Frohnapfel
Institute of Fluid Mechanics (ISTM)
Karlsruhe Institute of Technology
Kaiserstraße Karlsruhe 76131
carola.schmidt@kit.edu

ABSTRACT

While the impact of homogeneous roughness on wall-bounded turbulence is established to be similar between turbulent channel and boundary layer flows (Chung *et al.*, 2021), this similarity and thus transferability of obtained physical understanding is not obvious for heterogeneous rough surfaces. The heterogeneous roughness investigated here is that of a checkerboard arrangement of smooth and rough surface sections whose dimensions exceed the outer length scale of the flow. The turbulent flow fields that emerge over such a heterogenous rough surface are investigated and compared between turbulent channel flow and turbulent boundary layer. In both cases, it is observed that flow heterogeneity remains confined to a very near-wall region despite the large characteristic scale of the checkerboard pattern relative to the outer scales of the flows. The flow heterogeneity appears to increase in strength with increasing Reynolds number.

Introduction

The effect of rough surfaces on a fluid and its drag is of key interest within fluid dynamics. While the classical reference data for rough surfaces were obtained in pipe flows (see Nikuradse or Moody plots) the corresponding impact can be translated to boundary layer flows due to the well-established similarity in near-wall turbulence. Heterogeneity of roughness occurs in real-world scenarios, both in natural and artificial structures. While its relevance is clearly observed, there is no clear-cut definition of heterogeneous roughness and different realizations of heterogeneity can be thought of (Jensen & Forooghi, 2025). For the present study, we consider a heterogeneous roughness which is built by two subsurfaces: smooth wall and sandpaper. Both subsurfaces constitute 50 % of the total surface and are arranged in a checkerboard pattern.

Previous studies on non-homogeneous roughness have mostly concentrated on two simplified configurations in which the step-change of smooth to rough occurs either along lines in streamwise or spanwise flow direction only. Longitudinally aligned strips of roughness were widely investigated, both in channel (Hinze, 1967) and boundary layer flow (Wangsawijaya *et al.*, 2020), and are known to introduce turbulent secondary motions, which leave a characteristic footprint on the streamwise mean flow. Turbulent secondary motions are understood to carry rather similar properties in channel flows and boundary layers (Vanderwel *et al.*, 2019). A spanwise aligned step change in surface property was mostly investigated in boundary layers and has been observed to cause the formation of an internal boundary layer (Bou-Zeid *et al.*, 2004). There is a clear difference in flow field response for internal flows since any change in the near-wall flow field in form of flow acceleration or deceleration is accompanied by changes in the full flow field due to continuity (Van Buren *et al.*, 2020).

The checkerboard pattern of the present work combines these two configurations of streamwise and spanwise step-changes. Pressure drop measurements in a channel flow facility revealed a surprisingly low flow resistance of the checkerboard pattern, which between $Re_b = 10,000$ and $Re_b = 20,000$ reaches a more than 10 % lower friction coefficient than reference cases in which roughness is introduced in form of streamwise or spanwise strips (Sujar-Garrido *et al.*, 2025). In the channel flow configuration it was found that the degree to which the checkerboard surface pattern transfers its spatial heterogeneity to the flow field depends on Reynolds number (Schmidt *et al.*, 2026). The present work aims to investigate whether a similar dependence of flow field heterogeneity on Reynolds number can also be found in turbulent boundary layers.

Experimental Set-up and Methodology

The checkerboard pattern is realized by P60 sandpaper alternating with a smooth wall. It has patch dimensions of $s^2 = 50\,\text{mm} \times 50\,\text{mm}$. For the channel flow investigation, this pattern was realized on plates that are 300 mm wide. An image of this plate under the laser sheet can be seen in figure 1 (a). Additional reference plates are a polished aluminium wall,

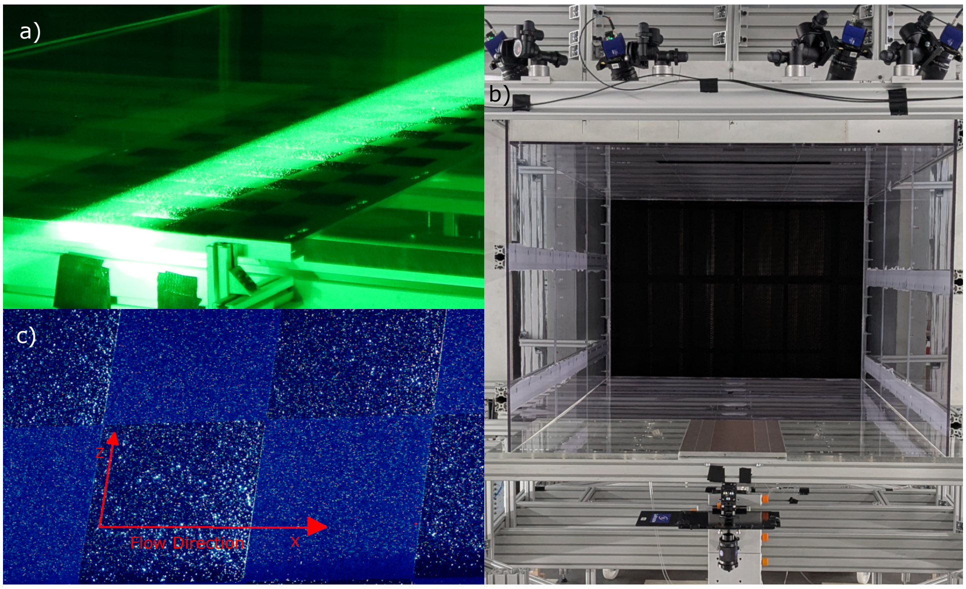

Figure 1: (a) The laser volume above the checkerboard roughness. (b) The experimental setup in the boundary layer wind tunnel and the overhead cameras. (c) An example of an unprocessed particle image above the checkerboard roughness.

and a homogenously rough P60 sandpaper wall (the same two materials that make up the squares in the checkerboard roughness). Sandpaper was inset into the plates such that the mean surface height was the same for the rough and smooth walls. In the boundary layer study, the roughness plates are placed into a zero pressure gradient turbulent boundary layer (TBL) which initially evolves over a smooth surface. Boundary layer thickness varied between $\delta_{99} = 23.7\,\text{mm}$ and $\delta_{99} = 29.1\,\text{mm}$ at the beginning of the tested roughness plates, dependent on U_∞. These values are used as reference boundary layer thickness for normalization of the results. They are similar to the channel height in the channel flow experiments which is given by $H = 2h = 25.4\,\text{mm}$. The PTV measurements in the TBL are taken in a volume centred approximately 500 mm downstream of the start of the roughness plates. Measurements in the boundary layer are taken at three different Reynolds numbers, with Reynolds number defined as $Re_\theta = \frac{U_\infty \theta}{\nu}$. Here, U_∞ is the freestream velocity, θ the momentum thickness at the beginning of the tested plates ($X = 0$), and ν the kinematic viscosity. The boundary layer parameters at the start of the rough surface section are summarized in table 1.

Table 1: Boundary layer reference parameters

Re_θ	θ (mm)	δ_{99} (mm)	U_∞ (m s^{-1})
1420	3.71	29.1	6.0
2510	3.30	25.7	12.0
3410	2.98	23.7	18.0

In the channel flow facility Reynolds number is defined as the bulk Reynolds number $Re_b = \frac{U_b H}{\nu}$, in which U_b is the bulk velocity, H is the channel height, and ν is the kinematic viscosity. In the turbulent channel flow hot-wire measurements are taken with a DANTEC 55P11 single hot-wire probe equipped with a tungsten wire with a diameter of 0.5 mm and a sensing length of 1.25 mm. The single point hot-wire measurement provides the streamwise velocity component (measured in the channel flow facility). Those are complemented with two particle tracking velocimetry (PTV) experimental campaigns (one in the channel and one in the boundary layer flow) that allow access to the full flow field in the measurement volume.

In the channel flow, time-resolved particle tracking velocimetry (TR-PTV) is recorded at 30 kHz. In contrast, the wind tunnel multi-pulse particle tracking velocimetry (MP-PTV) study acquires non time-resolved results at 15 Hz for the TBL case. Limitations on the high speed equipment setup means that the TR-PTV data is only captured over a volume of $18 \times 5 \times 10\,\text{mm}^3$ in the streamwise, wall-normal, and cross-stream directions. These directions are referred to here as X, Y, and Z respectively, with corresponding U, V, and W velocity components. The X, and Z directions are visible in figure 1 (c), while Y is towards the camera. The volume of MP-PTV data has larger limits of $125 \times 10 \times 76\,\text{mm}^3$. Distances along the checkerboard axis (X, and Z directions) are normalised using the square side length $s = 50\,\text{mm}$. The origin is always taken to be on the wall at the start of the roughness plate, on the centerline in cross-stream direction.

For TR-PTV, image acquisition is carried out using four Phantom v1840 cameras at 30 kHz. The flow is illuminated using a Photonics Industries high speed laser. The flow is passively seeded using water-based fog particles. In the case of MP-PTV (TBL in wind tunnel), image acquisition is carried out using four LaVision Imager CX12 cameras recording at 15 Hz. These can be seen suspended above the flow in figure 1 (b). The measurement area is illuminated using two Evergreen dual pulse lasers, which are overlapped to create a four pulse system. In both cases, cameras are suspended above the flow to acquire dense data without exceeding the particle per pixel limit of the shake the box algorithm (Novara *et al.*, 2016). In all MP-PTV cases, data is acquired between 1.4 mm and 10 mm above the wall surface, with one set of measurements (for the checkerboard case) reaching 0.5 mm from the mean surface height, or roughly 0.1 mm above the sandpaper peaks. Visual artifacts limit data acquisition in certain areas (visible in figure 1 (c)).

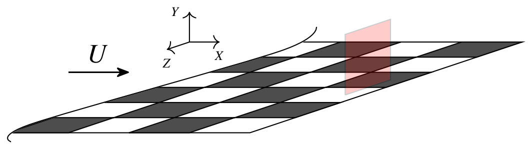

(a) Position of the measurement plane above the checkerboard pattern. The measurement plane is placed 30 mm $= 0.6s$ behind the step change.

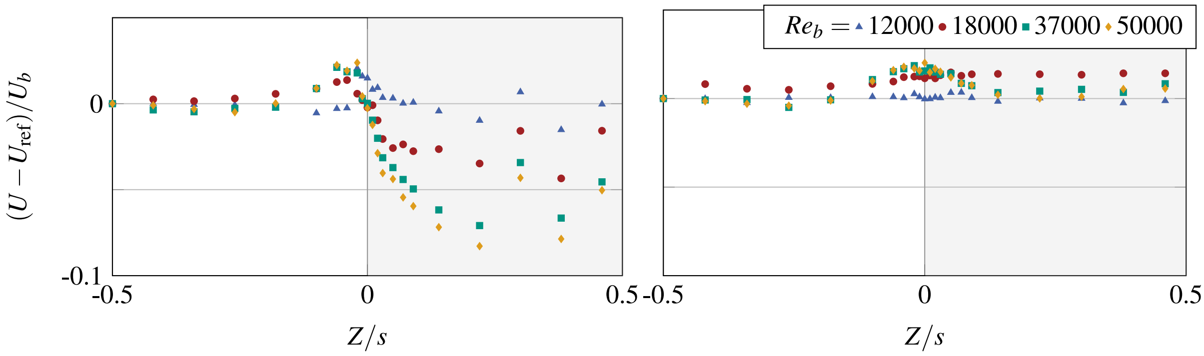

(b) $Y/h = 0.06$

(c) $Y/h = 0.6$

Figure 2: Profiles of normalised velocity deviation ($\frac{U-U_{\text{ref}}}{U_b}$) above the checkerboard roughness, U_{ref} refers to the velocity in the centre of a smooth patch at the current height and bulk velocity (U_b). Figure (a) is a diagram showing the location of the plane from which these profiles are taken. This data is taken using hot-wire annemometry (HWA) in the channel flow facility at a variety of Re_b values. These profiles are in the cross-stream (Z) direction at $X/s = 0.6$ behind a square transition, the positive Z direction shows the flow above a rough square, while the negative Z direction shows the flow above a smooth square. Figure (b) shows profiles at a height of $Y/h = 0.06$, while figure (c) shows profiles at a height of $Y/h = 0.6$.

Results

Figure 2a shows the measurement location for the hot-wire measurements in the channel flow. It is located 30 mm behind the step change in surface property. Measurements of the streamwise mean-flow component are taken at two different wall-normal positions ($Y/h = 0.06$, and $Y/h = 0.6$) and the corresponding results are shown in figure 2 (b). Here, the positive Z direction shows the flow above a rough patch, while the negative Z direction corresponds to the flow above a smooth patch. The data is plotted in terms of a normalised velocity deviation from a reference velocity U_{ref} located at the center of the smooth patch. Normalisation is based on the bulk velocity U_b of the channel flow. Results are presented at four different bulk Reynolds numbers Re_b.

Close to the wall (figure 2 (b)) stronger relative variations of the streamwise mean velocity are observed than at larger wall distance (figure 2 (c)). In general, the near-wall flow over the rough patch is slower than over the smooth one, except for the lowest Re_b where similar values of U are measured in the center of the smooth and the rough patch. The flow-field heterogeneity in the near-wall region ($Y/h = 0.06$) is observed to clearly increase in magnitude with increasing Re_b for the two intermediate Reynolds numbers and shows less changes in the range of $Re_b = 37,000 - 50,000$. All higher Re_b-cases reveal a peak of U at the edge of the smooth surface section. This peak is also visible at larger wall distance ($Y/h = 0.6$) for all cases except the lowest Re_b-case. At this larger wall distance, little heterogeneity, or Reynolds number dependence is visible. At this height, spanwise variation does not exceed 2.5% of U_b, and does not follow any clear trend with respect to Reynolds number.

Figure 3 shows a comparison of datasets from differing measurement techniques and flow facilities. In order to make channel-flow data comparable with boundary layer measurements, channel flow velocities are normalised using the centreline velocity (U_c), and vertical lengthscales are normalised using the channel half-height (h). Whereas; boundary-layer measurements are normalised using the freestream velocity (U_∞), and the reference boundary layer depth (δ_{99}) at the beginning of the roughness plate. In both cases horizontal and streamwise distances are always normalised using the checkerboard square size (s =50 mm).

All sub-figures in figure 3 are measured behind a square transition, such that the positive Z direction is $0.1s$ in the wake of a smooth square. Figures 3 (a), (b), and (c), all show iso-contours of streamwise velocity moving closer to the surface on the positive Z side, relative to the negative Z side (the wake of the rough patch). These findings are consistent with the velocity increase in wall parallel plane that can be observed in figure 2. The near-wall flow behaviour over the roughness patches is thus found to be similar for turbulent channel flows and turbulent boundary layers.

In order to obtain an impression of the impact of the checkerboard surface on the boundary layer development, velocity profiles of the TBL over a smooth surface, a homogeneous rough sandpaper surface and the checkerboard configuration are compared at two different free stream velocities in figure 4. Note that the near-wall region over the checkerboard surface was measured in a separate campaign. This data is not available for the smooth and homogeneous rough surfaces. For $U_\infty = 6\,\text{m/s}$ little variation across the three cases is found. In contrast, at $U_\infty = 18\,\text{m/s}$ clear differences are visible. This is in agreement with the general understanding that the impact of roughness increases with increasing Reynolds number. The additional drag of the rough surface slows down the streamwise flow such that the achieved velocities at a given wall-

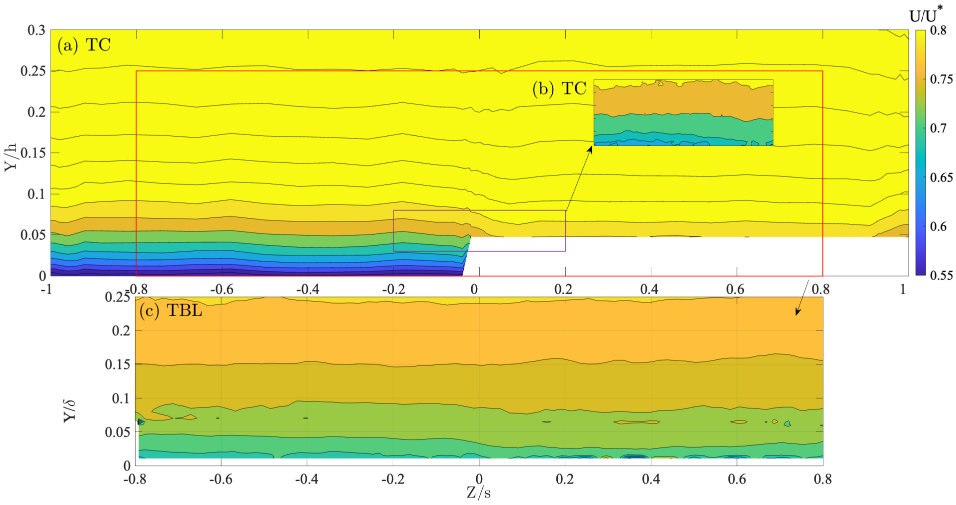

Figure 3: A comparison of measurement techniques and observations in the wake of a roughness transition above the checkerboard roughness. HWA data is taken $0.1s$ behind a transition, PTV data is averaged in the X direction across a volume between $X/s = 0.075$ and $X/s = 0.125$ behind a transition. Figure (a) shows HWA measurements taken in a turubulent channel flow facility (TC) at a Re_b of 18000. Figure (b) shows a small window of TR-PTV data, both this and figure (a) are normalised in the vertical direction by the half channel height (h =25 mm), and velocity is normalised by the channel centerline velocity. Figure (c) shows a measurement in the same position on the checkerboard but taken using MP-PTV in a boundary layer wind tunnel, in this case the vertical coordinate is normalised by the boundary layer depth (δ_{99}) and the velocity is normalised by U_∞. This figure is made up of two stitched datasets, these approximately cover the area above and below $Y/\delta_{99} = 0.06$. Some small visual artifacts are visible along this line.

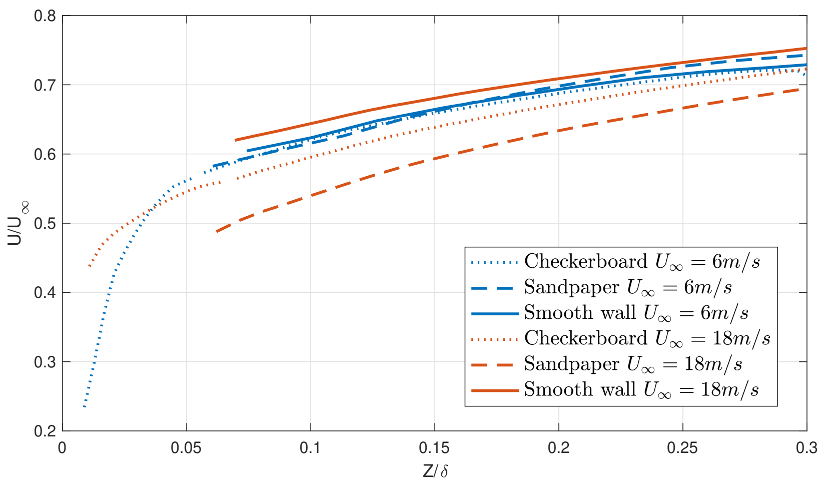

Figure 4: Vertical profiles of normalised streamwise velocity (U/U_∞) above the checkerboard and reference roughnesses. The highest and lowest velocities measured (6 and 18 m/s) are shown for comparison. This data was acquired using MP-PTV in the boundary layer wind tunnel. This profile was averaged between $X/s = 11.2$, $X/s = 11.8$ in the streamwise direction, and $Z/s = 0.4$ to $Z/s = -0.4$ in the cross-stream direction. In the checkerboard cases this was done with an equal weighting to the areas above smooth and rough walls.

normal distance are reduced. As expected, the velocity profile of the checkerboard surface (which is only partially rough) is located between the two reference cases.

In contrast to the hot-wire data, the PTV data provides access to the near-wall flow field over the full checkerboard structure. One example of the normalized mean streamwise-velocity in an $X-Z$-plane at $Y/\delta_{99} = 0.03$ is shown in figure 5 for three different U_∞ in the TBL. They all show distinct flow field heterogeneities which can only be detected up to a height of $y/\delta_{99} = 0.06$ above the checkerboard surface. The flow field heterogeneity appears to increase with increasing Reynolds number, in agreement with observations in turbulent channel flows (Schmidt *et al.*, 2026). In figures 5 (b) and (c) it can be seen that the streamwise flow velocity increases across the smooth patches, up to a peak near the transition to roughness. The flow velocity then decreases to a minimum near the transition back to a smooth wall. This acceleration-decceleration switch appears to happen very soon after the transition, at this Y location. At the highest freestream velocity the strength of this flow heterogeneity is up to 8% of U_∞.

Along this same plane the V velocity component shows no measurable heterogeneity for both the $U_\infty = 6\,\mathrm{m/s}$ and

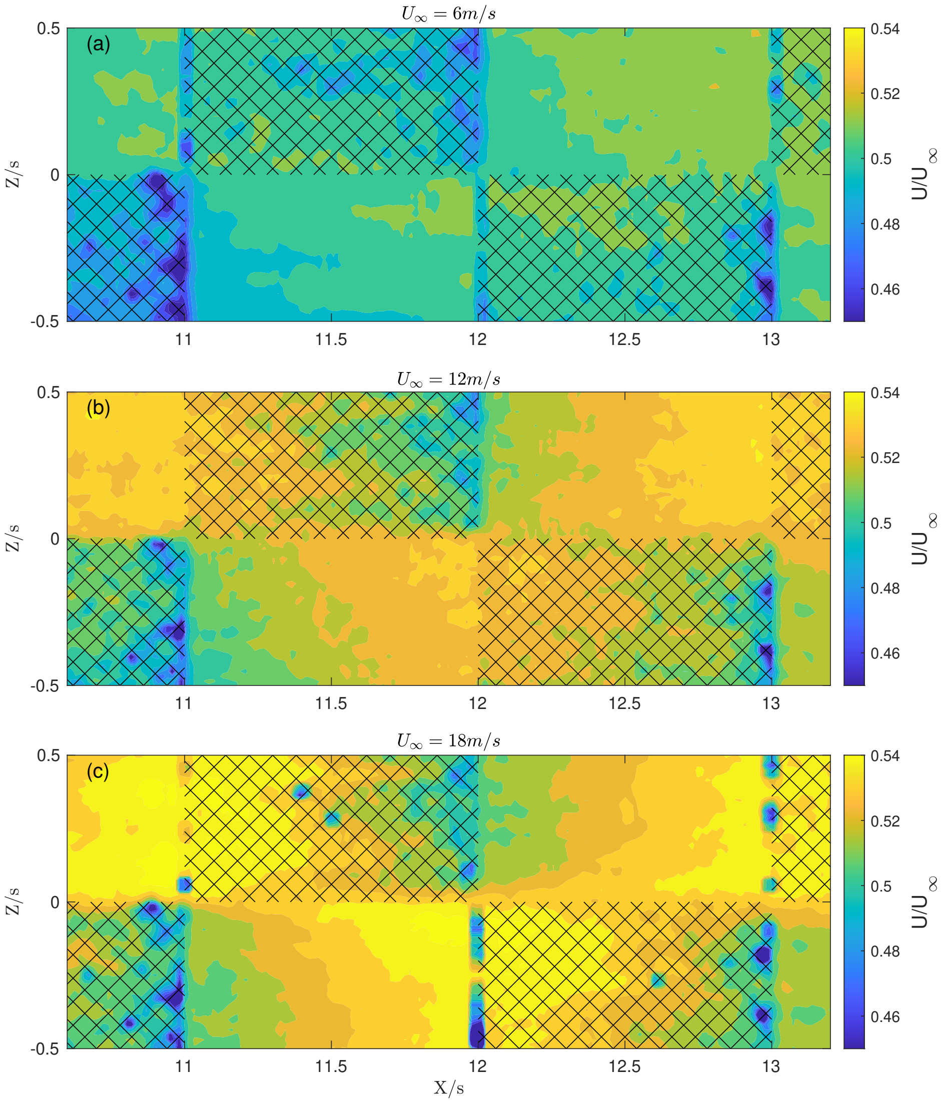

Figure 5: Near wall normalised streamwise velocity above the checkerboard roughness (U/U_∞) at $Y/\delta_{99} = 0.030$. Crosshatched squares indicate where the flow passes above a rough region of the checkerboard. Flow direction is left to right (positive X). This was measured using MP-STB in the boundary layer wind tunnel at three different free stream velocities $U_\infty = 6, 12, 18\,\text{m/s}$.

$U_\infty = 12\,\text{m/s}$ cases. The $U_\infty = 18\,\text{m/s}$ case shows a small upwards velocity above the rough patches and corresponding downwards velocity above the smooth patches. Even in the most heterogenous case, however, the magnitude of V is only of the order of 0.1% of U_∞. The W component of velocity in this plane is highly noisy relative to the other two. However, it can be seen that near the trailing edge of rough patches the W velocity is more likely to be in the direction of the neighbouring smooth patches. The strength of this velocity never exceeds 0.3% of U_∞ and is only present in the $U_\infty = 18\,\text{m/s}$ case. Hence, the fact that the surface heterogeneity translates more into flow heterogeneity with increasing Reynolds number is reflected in all mean velocity components.

The repeating formation of internal boundary layers, which can be understood as source of the flow inhomogeneity along a streamwise line, can also be seen in the Reynolds shear stress component $-\overline{u'v'}$ (Bou-Zeid *et al.*, 2004). This quantity is shown in normalised form in figure 6 for $U_\infty = 6\,\text{m/s}$ and $18\,\text{m/s}$. The shown data is averaged in the cross-stream direction between $Z/s = 0.4$, and $Z/s = 0.6$. While some noise is present in the measurements shown in figure 6, it can still be seen that for the $U_\infty = 6\,\text{m/s}$ case the Reynolds shear stress does not vary as it crosses the checkerboard patches. Contrastingly; at $U_\infty = 18\,\text{m/s}$ an increased level of turbulence activity can be seen rising from the rough patch. As the flow then moves in positive X direction above a smooth patch, this high $-\overline{u'v'}$ region is shifted upwards as a new lower $-\overline{u'v'}$ region begins to form. It should be noted that this pattern does not propagate throughout the entire height of the boundary layer; however, it does propagate further in Y than the heterogeneity in U_∞ does.

Conclusions

The turbulent flow over a checkerboard heterogenous roughness is examined in a turbulent channel flow (TC) and a turbulent boundary layer (TBL). In both cases, the side length (s) of the checkerboard roughness exceeds the outer scales of

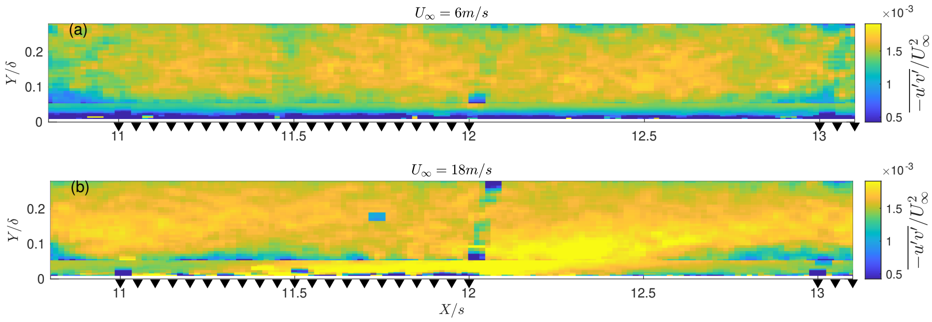

Figure 6: Internal boundary layer observed using $\overline{-u'v'}/U_\infty^2$. Both subfigures show this above checkerboard roughness at different U/U_∞, location of rough squares is indicated by textured x axis. Data is averaged from $Z/s = 0.4 - 0.6$. A visual artifact can be seen rising from $X/s = 12$, this is caused by missing data due to a bright line of background illumination. Artifacts can also be seen at approximatelly $Y/\delta_{99} = 0.06$, at which point high and low datasets are stitched.

the flow. Despite the structural heterogeneity being this large relative to the flow, the flow is highly homogenous. In both TC and TBL, heterogeneity of the mean flow field is limited to the very near-wall region and found to increase as Reynolds number increases. This near-wall flow field heterogeneity appears to be related to the repeated formation of internal boundary layers that are reflected in plumes of elevated Reynolds shear stress that are generated over rough surface sections and shifted away from the wall over the following smooth surface section.

The flow over the checkerboard pattern consistently shows an accelerating U velocity component over smooth patches and deceleration over the rough patches. It appears as if the rough patches act as obstacles to the flow in the sense that a small spanwise velocity component towards the smooth patches can be detected.

To conclude; checkerboard roughness can be described as roughness strips varying in both cross-stream and streamwise direction. In the measurements carried out here there is evidence of both cross-stream and stream-wise flow heterogeneity which appears, or strengthens, with increasing Reynolds number, both in TBL and in TC. The flow field heterogeneity remains confined to the near-wall region in both flow configurations. The one effect of stream-wise aligned strips, that is notable in its absence, are the large scale secondary motions that form along roughness boundaries (Hinze, 1967). This is unsurprising as they have been observed to require a significant development length (Hwang & Lee, 2018; Andreolli *et al.*, 2025). The impact of a checkerboard heterogeneous roughness on the flow resistance of a turbulent boundary layer remains to be investigated.

Acknowledgments

Financial support by the Deutsche Forschungsgemeinschaft (DFG, German Research Foundation) through project number 513183059 and the Struktur- und Innovationsfonds Baden-Württemberg (SI-BW, structural and innovation funds of Baden-Wuerttemberg) for the laser-optical measurement equipment is gratefully acknowledged. In addition, TR and PS acknowledge support through the Alexander von Humboldt Foundation.

REFERENCES

Andreolli, A, Hutchins, N, Frohnapfel, B & Gatti, D. 2025 Temporal decay of secondary motions in turbulent channel flows. *Journal of Fluid Mechanics* **1007**, A19.

Bou-Zeid, E, Meneveau, C & Parlange, M B. 2004 Large eddy simulation of neutral atmospheric boundary layer flow over heterogeneous surfaces: Blending height and effective surface roughness. *Water Resources Research* **40** (2).

Chung, D, Hutchins, N, Schultz, M P & Flack, K A. 2021 Predicting the drag of rough surfaces. *Annual Review of Fluid Mechanics* **53** (1), 439–471.

Hinze, JO. 1967 Secondary currents in wall turbulence. *The Physics of Fluids* **10** (9), S122–S125.

Hwang, H G & Lee, J H. 2018 Secondary flows in turbulent boundary layers over longitudinal surface roughness. *Physical Review Fluids* **3** (1), 014608.

Jensen, R M & Forooghi, P. 2025 A study of turbulent flow over patchy roughness. *Journal of Fluid Mechanics* **1067**.

Novara, M, Schanz, D, Reuther, N, Kähler, C J & Schröder, A. 2016 Lagrangian 3d particle tracking in high-speed flows: Shake-the-box for multi-pulse systems. *Experiments in Fluids* **57**.

Schmidt, C, Sujar-Garrido, P, Schmitgen, U & Frohnapfel, B. 2026 Influence of reynolds number on the pressure drop gradient of turbulent channel flow with heterogeneous roughness. *Journal of Fluid Mechanics* **Accepted for publication**.

Sujar-Garrido, P, Schmidt, C, Schmitgen, U, Leister, R & Frohnapfel, B. 2025 Friction coefficient and flow dynamics of a heterogeneously rough surface. 2nd European Fluid Dynamics Conference Dublin.

Van Buren, T, Floryan, D, Ding, L, Hellström, LHO & Smits, AJ. 2020 Turbulent pipe flow response to a step change in surface roughness. *Journal of Fluid Mechanics* **904**, A38.

Vanderwel, C, Stroh, A, Kriegseis, J, Frohnapfel, B & Ganapathisubramani, B. 2019 The instantaneous structure of secondary flows in turbulent boundary layers. *Journal of Fluid Mechanics* **862**, 845–870.

Wangsawijaya, D D, Baidya, R, Chung, D, Marusic, I & Hutchins, N. 2020 The effect of spanwise wavelength of surface heterogeneity on turbulent secondary flows. *Journal of Fluid Mechanics* **894**, A7.